Article

Characteristics of the Total Suspended Matter Concentration in the Hongze Lake during 1984–2019 Based on Landsat Data

Chenggong Du [1,2,3], Yunmei Li [4], Heng Lyu [4], Kun Shi [5,*], Naisen Liu [1,2,3], Chen Yan [1], Jinheng Pan [1], Yulong Guo [6] and Yuan Li [7]

[1] Jiangsu Collaborative Innovation Center of Regional Modern Agriculture & Environmental Protection, Huaiyin Normal University, Huaian 223300, China; ducg@hytc.edu.cn (C.D.); boomzip@hytc.edu.cn (N.L.); 1901190038@stu.hytc.edu.cn (C.Y.); 1901190019@stu.hytc.edu.cn (J.P.)
[2] Jiangsu Key Laboratory for Eco-Agricultural Biotechnology around Hongze Lake, Huaiyin Normal University, Huaian 223300, China
[3] Jiangsu Engineering Research Center for Cyanophytes Forecast and Ecological Restoration of Hongze Lake, Huaiyin Normal University, Huaian 223300, China
[4] Key Laboratory of Virtual Geographic Environment of Education Ministry, Nanjing Normal University, Nanjing 210046, China; liyunmei@njnu.edu.cn (Y.L.); heng.lyu@njnu.edu.cn (H.L.)
[5] Nanjing Institute of Geography and Limnology, Chinese Academy of Sciences, Nanjing 210008, China
[6] College of Resources and Environment, Henan Agricultural University, Zhengzhou 450002, China; gyl.zh@henau.edu.cn
[7] School of Tourism and City Management, Zhejiang Gongshang University, Hangzhou 310000, China; liyuan@mail.zjgsu.edu.cn
* Correspondence: kshi@niglas.ac.cn; Tel.: +86-182-6000-2994

Abstract: The Hongze Lake is the fourth largest freshwater lake in China and an important lake for the East Route of the South-to-North Water Diversion Project. The water quality of the lake affects social development and the lives of residents. To assess the impacts of environmental changes and human activities on the distribution of the total suspended matter (TSM) in the Hongze Lake, we developed an algorithm that utilizes the near-infrared (NIR) band to estimate TSM based on in situ measurements. The algorithm was applied to Landsat images to derive TSM distribution maps from 1984 to 2019, revealing significant inter-annual, seasonal, and spatial variability. The relationship between TSM, precipitation, and wind speed was analyzed, and we found that: (1) The estimation model of TSM concentration in the Hongze Lake constructed for TM and OLI has a high accuracy, and it can be used to jointly monitor TSM concentration in the Hongze Lake for long-term series; (2) From 1984 to 2019, the concentration of TSM in the Hongze Lake showed a trend of first rising and then falling, with the maximum value in 2010 at 100.18 mg/L mainly caused by sand mining activities. Precipitation and wind speed weakly influence the inter-annual variation of TSM concentration; (3) The concentration of TSM in the Hongze Lake in summer is easily affected by flooding in the Huai River, and the concentration of TSM in other seasons is significantly negatively correlated with precipitation; (4) TSM is highest in the Huaihe Bay, followed by the Lihe Bay and Chengzi Bay. The main reason for this is that the input of the Huaihe Bay flows directly into this lake area and is also the main navigation channel. The results of this study are of great significance for the protection and management of the water environment of the Hongze Lake.

Keywords: Hongze Lake; total suspended matter; remote sensing; driving factors

1. Introduction

The fourth largest freshwater lake in China, the Hongze Lake, is located in the northern part of the Jiangsu Province. The Hongze Lake has multiple functions, such as flood control, drinking water supply, irrigation, shipping, aquaculture, and biodiversity maintenance. It is also a main water transmission line and the water storage body for the "South-to-North Water Transfer" East line project [1,2]. The changing water quality of the Hongze

Lake is directly related to the water quality safety of the South-to-North Water Diversion Project and is, therefore, of great significance for the economic and ecological sustainable development of the surrounding area and the entire Huai River Basin.

Total suspended matter (TSM) refers to substances suspended in water that exceed a certain size. TSM includes inorganic matter, organic matter, silt, clay and microorganisms that are insoluble in water [3,4]. In inland water, the river input adds large amounts of TSM to lakes [5]. Terrestrial nutrients are easily adsorbed onto the suspended particles and enter the lake, promoting the eutrophication of water bodies and the outbreak of water blooms [6,7]. Moreover, TSM affects the optical signal of inland water bodies, which has an important impact on the growth of aquatic animals and plants [4,8,9]. TSM content is an important indicator for measuring water clarity and the degree of water pollution. Therefore, the rapid and accurate monitoring of the TSM concentration in water bodies is important for controlling the water pollution. There are many farmlands around the Hongze Lake; therefore, surface pollution also decreases the water quality. Additionally, the Huai River, the largest river flowing into the lake, brings large amounts of sediment into the Hongze Lake every year. Moreover, long-term sand mining activities have led to an increase in TSM concentration in the Hongze Lake and have caused the further deterioration of water quality [10]. Therefore, the concentration of TSM in the Hongze Lake must be accurately monitored.

Unlike conventional water quality monitoring methods, remote sensing can monitor a wide range of quality parameters in real time, saving time and effort [11–14]. Remote sensing has been widely used in monitoring water bodies, including water quality parameter inversion and cyanobacteria bloom monitoring [15–21]. Among them, the common water quality parameters that can be accurately estimated are chlorophyll a (chl-a) levels, TSM, color dissolved organic matter (CDOM), and turbidity [22–27]. As a suspension of water-based optically active substances, TSM can be effectively monitored using remote sensing technology [28–30]. Research results have been obtained for the remote sensing estimation of TSM concentration in inland waters, which are mainly divided into analytical algorithms, semi-analytical algorithms, and empirical algorithms. The remote sensing data used mainly include MODIS, VIIRS, Landsat series, GOCI, MERIS, Sentinel, and Gaofen series [3,8,31–36]. Empirical models can be subdivided into fitting and machine learning algorithms. For multi-spectral data and specific research areas, the empirical method is simple and fast, and the estimation accuracy meets the needs of remote sensing monitoring, and is more suitable for the processing and application of large time scales and big data [10,32,37].

The long-term analysis of the concentration of water quality parameters is helpful for understanding the trend of water quality changes, and provides an important reference for the treatment and protection of the water environment. The long-term continuous monitoring of the TSM concentration in the Hongze Lake is helpful for understanding the trends and characteristics TSM concentration at different time-points and areas. Furthermore, such monitoring can be combined with meteorological and human activities to identify the factors influencing changes in TSM concentrations. This study is expected to provide scientific data support for the protection and management of the water environment of the Hongze Lake. The Landsat series data presently have the longest time span of remote sensing data, and have been applied to the long-term change trend of water quality for other lakes. Currently, there is no algorithm for the long-term remote sensing estimation of the concentration of TSM in the Hongze Lake based on Landsat data, and whether the data estimation results of Landsat series data between different sensors are consistent is yet to be determined. Therefore, it is necessary to construct a remote sensing estimation model of TSM concentration suitable for the Hongze Lake using Landsat data and analyze the long-term temporal and spatial changes in the lake. It is urgently necessary for policy makers to develop suitable strategies to improve water quality.

The objectives of this study are to: (1) calibrate and validate the TSM estimation model using Landsat series data from the Hongze Lake, (2) reveal the long-term trend in TSM

variation, and (3) address the potential effects of climate change and human activities on TSM to improve future water quality management.

2. Materials and Methods

2.1. Study Area

The Hongze Lake is located between 33°06′–33°40′ N latitude and 118°10′–118°52′E longitude. It is a shallow water lake in the lower reaches of the Huai River in the western Jiangsu Province, Huai'an, and Suqian. The Hongze Lake undertakes the water of 158,000 km^2 in the upper and middle reaches of the Huai River. This area accounts for 83.6% of the Huaihe River Basin. It is the junction point of the middle reaches of the Huai River, tributaries, and downstream rivers. Water from the rivers enters the lake on the west and south sides, and water from the Huai River accounts for more than 70% of the total lake [38]. The Hongze Lake plays an important role in flood regulation in the lower reaches of the Huai River. Based on the characteristics of the different lake areas, the Hongze Lake can be divided into three lake bays. The Chengzi Bay is relatively closed. It is the main purse-breeding area in the Hongze Lake. The water exchange is slower, and the degree of eutrophication is higher. The Huaihe Bay is the main water passing area of the Hongze Lake. The water body is turbid, the lake disturbance is severe, and the suspended sediment content is high. The Lihe Bay is the main lake in the west. In the river distribution area, the water body has a strong self-purification ability and is mainly distributed in aquatic plants and aquaculture. Its eutrophication was lower than that of the Chengzi Bay. The study area and sampling sites were shown in Figure 1.
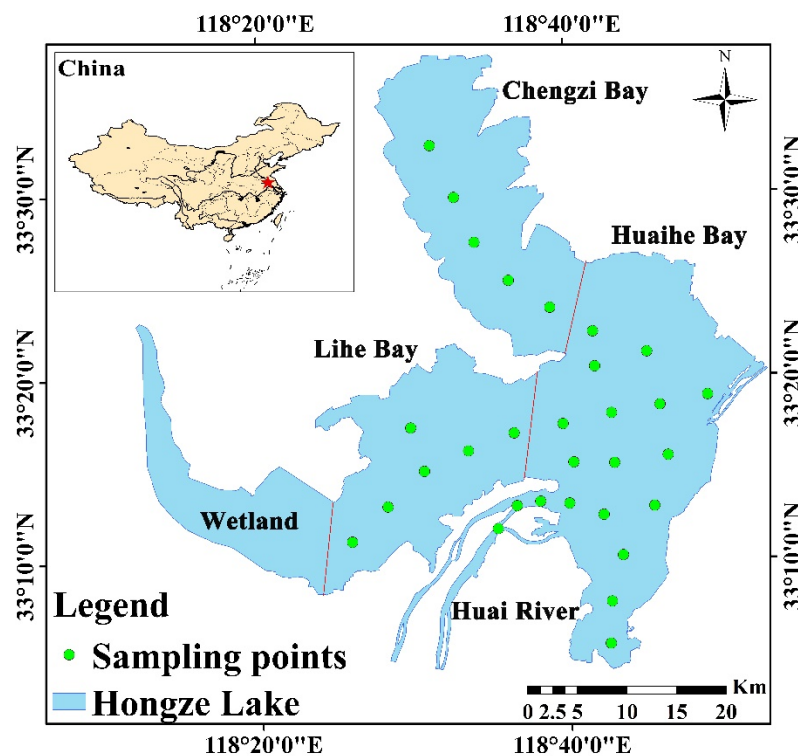
Figure 1. The study area and the distribution of sampling points.

2.2. In-Situ Data

The data used in this study are shown in Figure 2. R$_{rs}$ and TSM concentration were used to build a remote sensing estimation model of TSM concentration. The model was applied to Landsat series data to analyze the temporal and spatial distribution of TSM concentration in the Hongze Lake, and the influencing factors were analyzed in combination with meteorological and economic data.
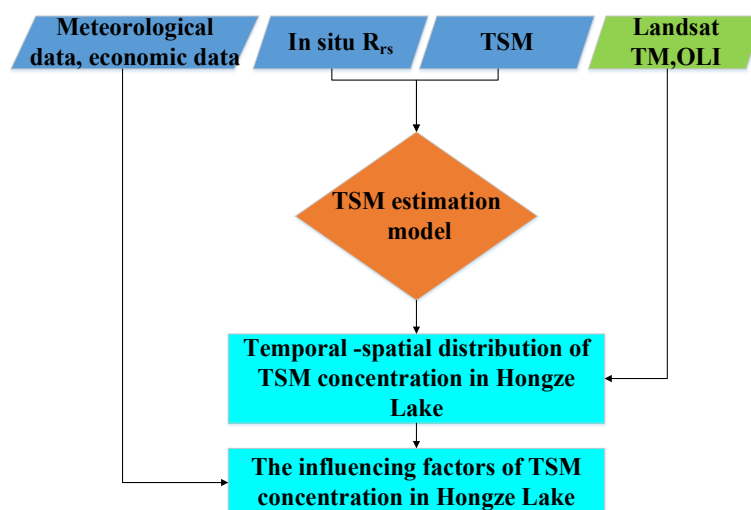
Figure 2. Flow chart of this study.

2.2.1. Spectral Data Collection

The water surface spectral data were acquired using an ASD Field Spec Pro portable spectrometer with a range of 350–1050 nm. The entire process measured the radiation information of a standard gray board, the water body, and light from the sky, and each parameter measured 10 spectra. R_{rs} (sr^{-1}) was calculated using the following equation [39]:

$$R_{rs}(\lambda) = \left(L_t - r \times L_{sky}\right) / \left(L_p \times \pi / \rho_p\right) \tag{1}$$

where L_t is the total radiance of the water surface; r denotes skylight reflectance at the air-water surface, and its value is affected by water-surface roughness caused by wind speed (2.2% for calm weather; 2.5% for <5 m·s^{-1} wind speed; 2.6–2.8% for about 10 m·s^{-1} wind speed); L_{sky} is the measured radiance from the sky; L_p is the measured radiance of the gray reference panel; and ρ_p is the reflectance of the gray diffuse panel.

2.2.2. Suspended Matter Concentration Measurement

Water samples were also collected from the surface and taken back to the laboratory for TSM measurement, which was conducted within less than 12 h. Water samples were filtered through Whatman GF/F fiberglass filters and weighed according to the method described in previous studies [32,40]. A total of 42 samples was collected in June 2018 and April 2019, of which 32 were used for modeling and 10 were used for verification. The concentration of TSM ranged from 11.53 mg/L to 86.80 mg/L, with an average value of 36.57 mg/L.

2.2.3. Meteorological Data

The meteorological data used in this study were obtained from China Meteorological Data Network (http://data.cma.cn/site/index.html/, accessed on 9 October 2021), which included the data from two meteorological stations (Sihong and Xuyi) in the Hongze Lake region from 1984 to 2019. The dataset included daily precipitation and daily average wind speed. The downloaded weather data were averaged monthly and annually; these time periods were consistent with the monthly and annual periods for which the average data of remote sensing images were obtained.

2.2.4. Economic and Demographic Data

The gross domestic product (GDP) data and population data of Huai'an city were selected to evaluate the impact of economic development on the water quality of the Hongze Lake, and relevant data were obtained from the Huai'an Bureau of Statistics (http://tjj.huaian.gov.cn/, accessed on 15 October 2021).

2.3. Satellite Data

Landsat series data, including Landsat 5 TM (1984–2011) and Landsat 8 OLI (2013–2019) data, were downloaded from https://earthexplorer.usgs.gov/ (accessed on 12 July 2021) and were used to retrospectively investigate the spatiotemporal variations in TSM. Because of the failure of the Landsat-7 ETM+ airborne scan line corrector (SLC), the data sourced from it were not used, and the 2012 image data were missing. Because the Landsat L1TP data were inter-calibrated across different Landsat sensors, L1TP data were consistent across the different Landsat sensors and suitable for pixel-level time series analysis [41]. A total of 172 cloud-free images of the Hongze Lake were collected from 1984 to 2019. The top-of-atmosphere radiance was obtained by radiometric calibration, and the water surface remote sensing reflectance was derived using the Fast Line-of-sight Atmospheric Analysis of Spectral Hypercubes (FLAASH) module, which is embedded in ENVI 5.3 software. The FLAASH atmospheric correction module was developed using Moderate Resolution Atmospheric Transmission (MODTRAN5) and is widely applied to various satellite sensors (e.g., Landsat TM, OLI, and HJ-1A/B CCD) over ocean, coastal, and inland water bodies [32,33,42]. Therefore, FLAASH was used to perform the atmospheric correction of Landsat TM and OLI images. In addition, the dimensionless FLAASH-corrected reflectance can be converted to remote sensing reflectance through division by the value of π [43]. The specific time of the Landsat images used is shown in Figure 3 and Table A1.
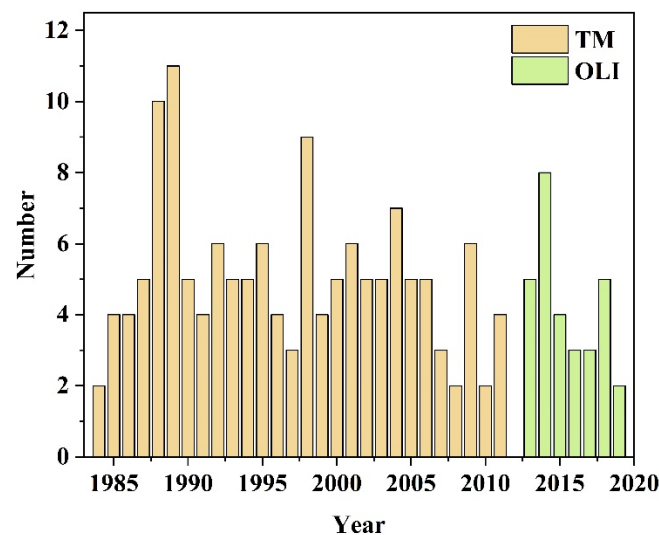
Figure 3. Valid Landsat images from 1984 to 2019. Gray and blue correspond to the year when TM and OLI have data, respectively.

2.4. Performance Evaluation

The accuracy of the inverse model was measured using the mean absolute percentage error (MAPE) and the root-mean-square error (RMSE). The two parameters were calculated as follows:

$$\text{MAPE} = \frac{1}{n}\sum_{i=1}^{n}|\frac{y_i - y_i'}{y_i}| \times 100\% \tag{2}$$

$$\text{RMSE} = \sqrt{\frac{1}{n}\sum_{i=1}^{n}(y_i - y_i')^2} \tag{3}$$

where y_i and y_i' are the measured and retrieved TSM, respectively.

3. Results

3.1. Development and Assessment of the TSM Retrieval Algorithm

For Landsat series data, the use of near-infrared bands to construct a single-band algorithm has been widely used in inland water bodies [32,44,45]. A long wavelength with high pure water absorption ensures that high TSM concentrations can be well estimated, avoiding the algorithm saturation expected at lower wavelengths, but with the disadvantage of reduced sensitivity to low concentrations. Therefore, this study uses the near-infrared band to construct a remote sensing estimation model of TSM concentration suitable for the long-term observation of the Hongze Lake based on Landsat series data. Although the Landsat series TM and OLI data band settings are similar, there is still a fine difference, so separate modeling is needed. First, the measured spectral data were fitted using a spectral response function. Next, the near-infrared band and measured TSM data were used for function fitting. The results were as shown in Figure 4: The fitting accuracy R^2 of the near-infrared band of Landsat 8 OLI data was 0.85, and the fitting accuracy of Landsat TM data was 0.86. Additionally, verification points were used to verify the accuracy of the model; MAPE was 17.74% and 16.48%, respectively, and the RMSE was 6.09 mg/L and 5.44 mg/L. The results show that the models constructed based on TM and OLI data were able to perform the high-precision inversion of the TSM concentration in the Hongze Lake to meet the application requirements. To ensure the consistency of the monitoring results of the OLI and TM data, the estimated results of the two datasets were compared and analyzed. Seen from Figure 5, the data are better distributed near the one-to-one line, indicating that the long-term serial analysis of the concentration of suspended solids in the Hongze Lake can be combined.

$$y = 4368.9x + 13.02 \; R^2 = 0.85 \tag{4}$$

where y and x are TSM and Landsat 8 OLI R_{rs} (NIR), respectively.

$$y = 3451.9x + 11.46 \; R^2 = 0.86 \tag{5}$$

where y and x are TSM and Landsat TM R_{rs} (NIR), respectively.

3.2. Spatial Change of TSM Concentrations in the Hongze Lake in the Past 36 Years

The constructed TSM remote sensing estimation models were applied to Landsat images from 1984 to 2019 to explore the 35-year suspended matter concentration changes in the Hongze Lake. The annual average result was obtained by averaging all the image data from one year. The results are presented in Figure 6. It is apparent that the concentration of TSM in the Hongze Lake had obvious inter-annual changes. From 1984 to 2006, the TSM concentration in the Hongze Lake showed a slow increasing trend. The maximum value was 63.92 mg/L in 1998. Subsequently, the concentration of TSM gradually decreased until 2006, and the average concentration of the whole lake dropped to 41 mg/L. Beginning in 2007, the concentration of TSM increased sharply and lasted until 2013, with the highest value being 100.18 mg/L in 2010. The concentration dropped sharply in 2014, and the concentration in the Hongze Lake was relatively low in 2019.

The concentration change trends for the three bays were relatively consistent in Figure 7. From 1984 to 2019, the concentration of TSM in the Huaihe Bay was the highest. It is worth noting that the higher concentrations of TSM in the Huaihe Bay often extend from the estuary of the Huai River to the outside. The individual pictures show that a line of high TSM concentration extends from the Huaihe Bay to the Hongze District. From 1984 to 2006, the concentration of TSM at the mouth of the Huaihe Bay showed a fluctuating pattern, with large changes from year to year, and no obvious upward trend overall. The maximum value was 73.9 mg/L in 1986, and the highest in the other two years were 68.48 mg/L and 70.99 mg/L in 1991 and 1996, respectively. Beginning in 2006, the concentration of TSM increased sharply, reaching a maximum value of 100.18 mg/L in 2010. The high value continued until 2013 and then began to decline. The concentration of TSM in the Lihe Lake

Bay fluctuated between 1984 and 2006. Compared with the Huaihe Lake Bay, the years of decline and increase were more consistent, but the inter-annual changes in concentration were subtle. Notably, in some years, the TSM concentration reached its lowest value in the three bays. From 2006 to 2013, TSM was also at a relatively high concentration. From 1984 to 2006, the concentration of TSM in the Chengzi Bay did not change significantly, and the overall concentration was relatively stable. However, by 2007, the concentration of TSM also rose sharply, and stayed at that level until 2013.
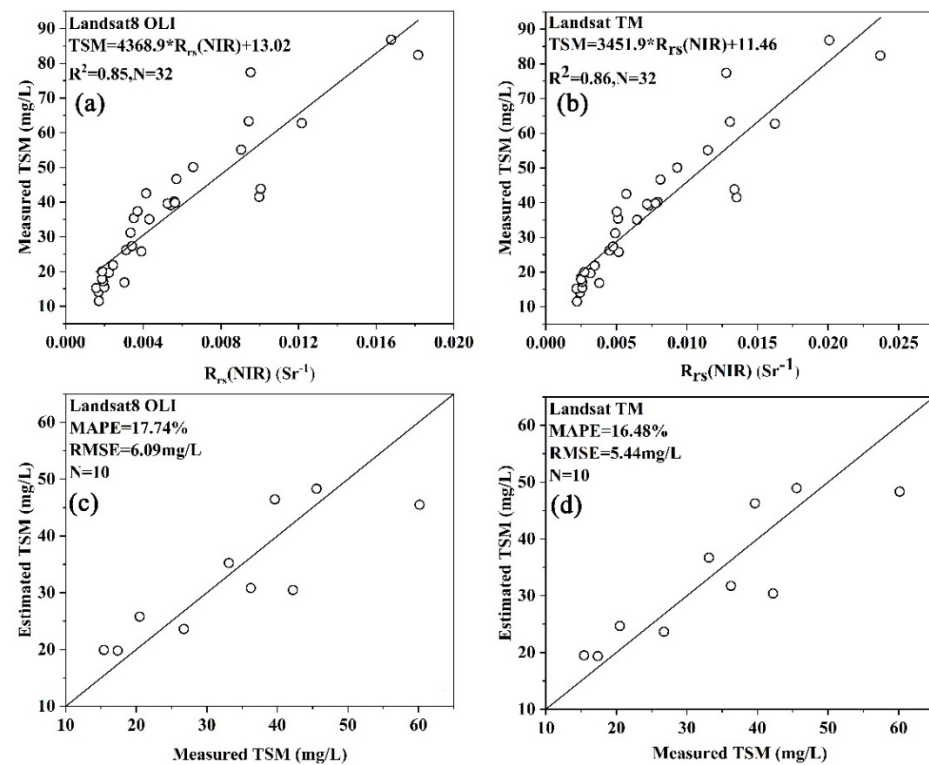
Figure 4. Fitting curve of TSM and Rrs for (**a**) Landsat 8 OLI and (**b**) Landsat TM; Comparing the estimated and measured TSM based on the validation data for (**c**) Landsat 8 OLI and (**d**) Landsat TM.
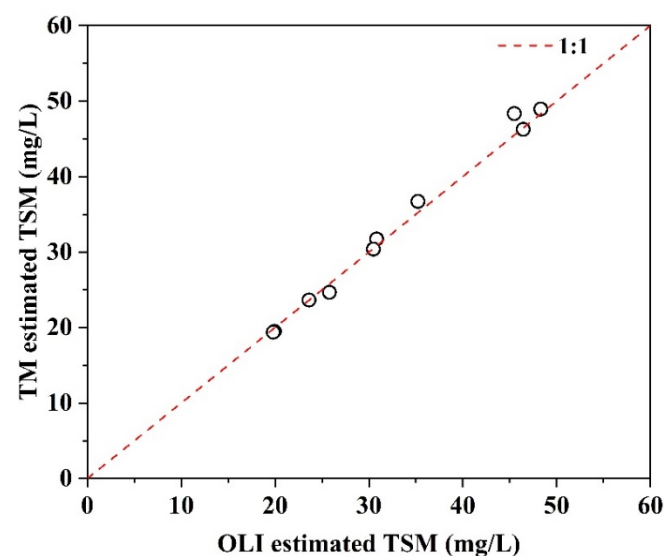
Figure 5. Comparing OLI-estimated TSM and TM-estimated TSM based on the validation data.
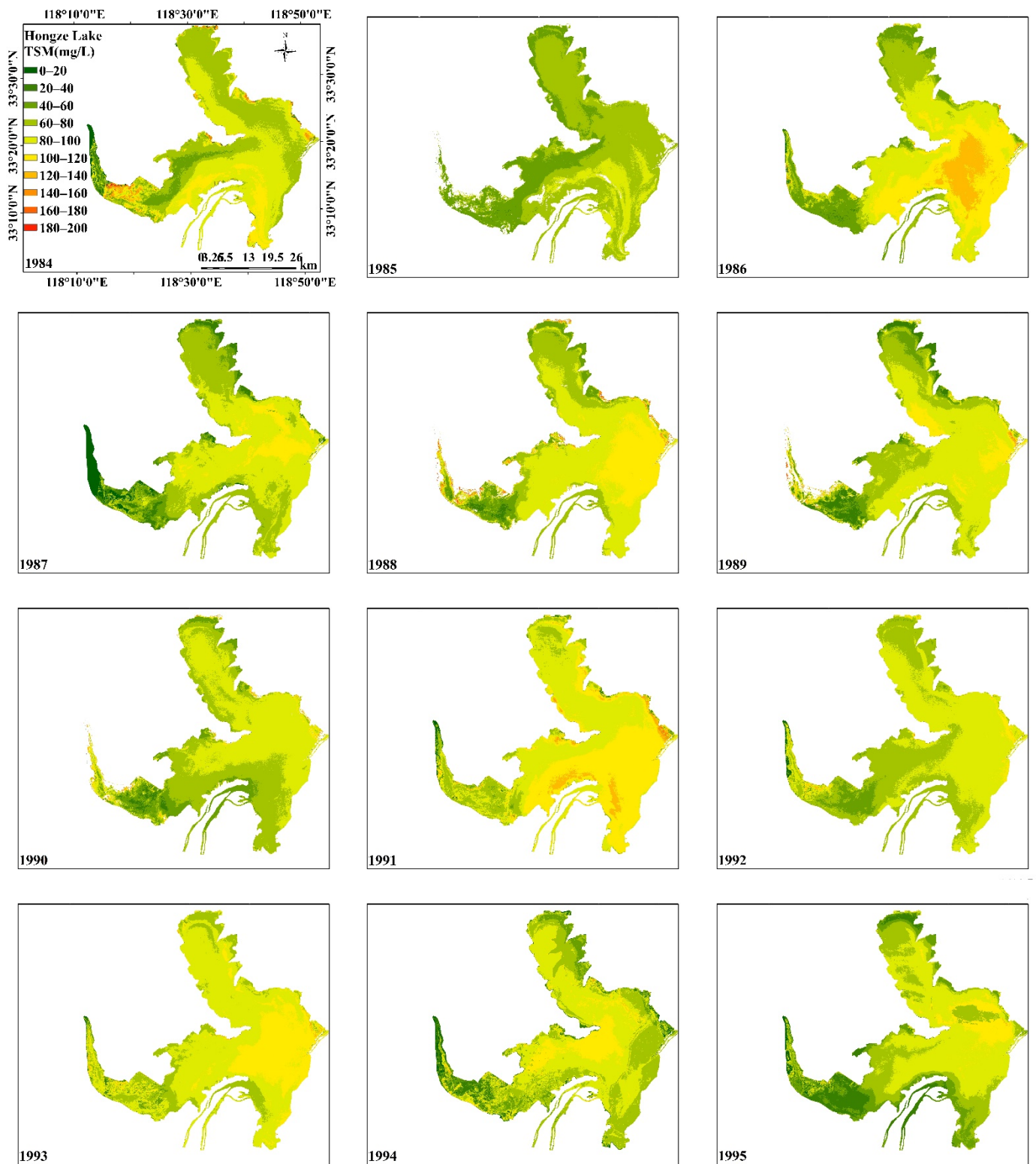
Figure 6. *Cont.*
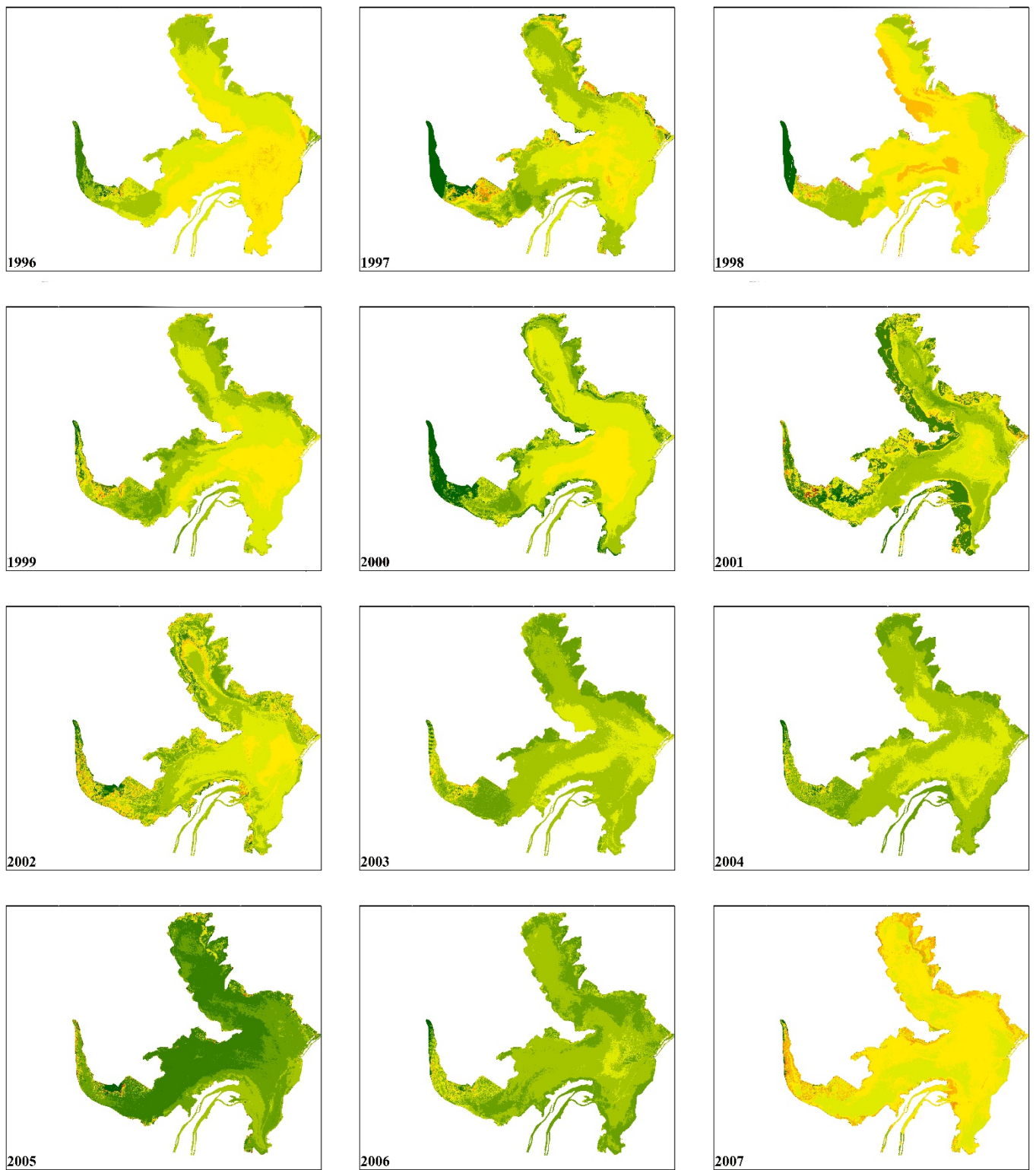
Figure 6. *Cont.*
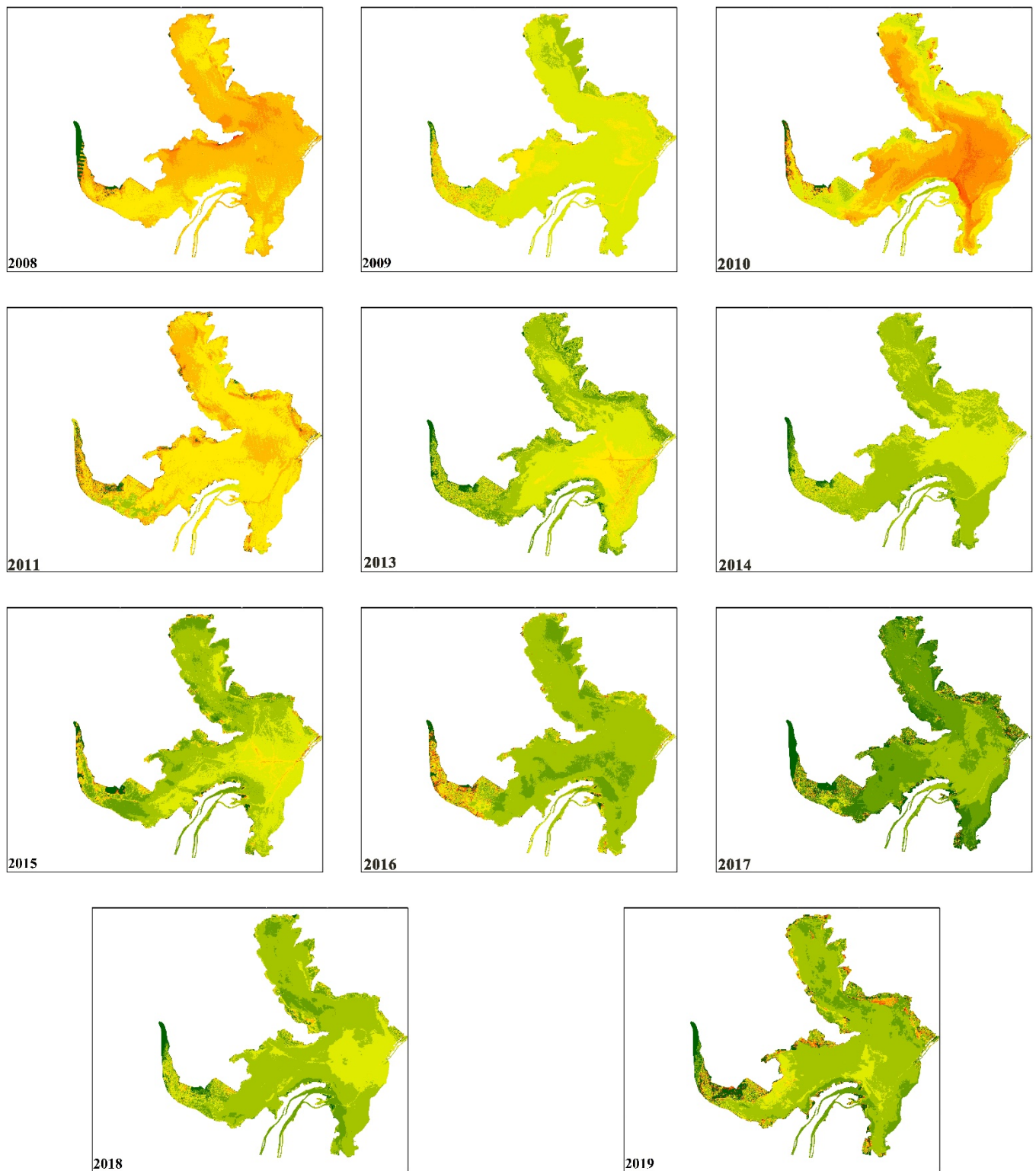
Figure 6. Inter-annual changes in the TSM concentration in the Hongze Lake from 1984 to 2019.
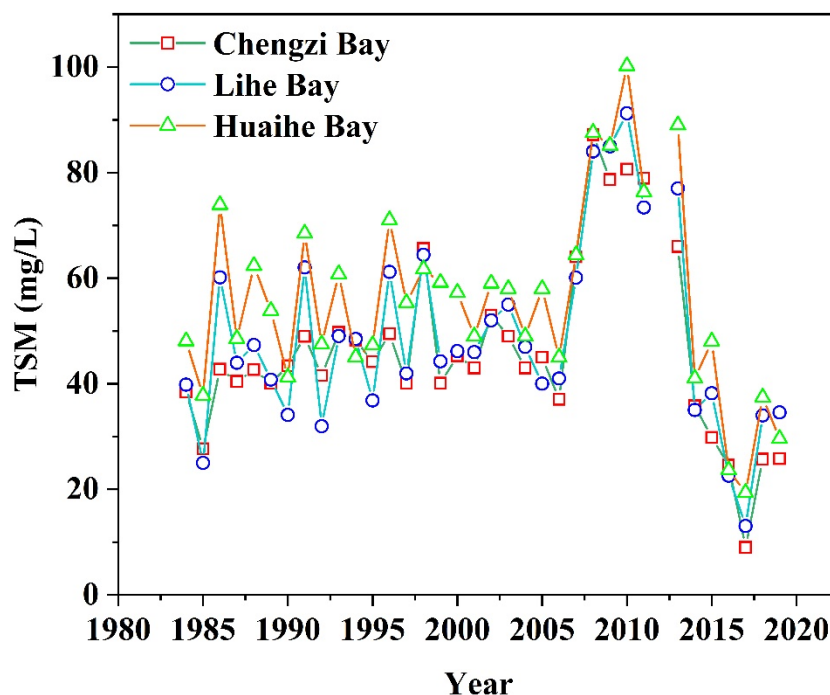
Figure 7. Line chart of TSM changes in the Chengzi Bay, Suhe Bay, and Huaihe Bay from 1984 to 2019.

3.3. Seasonal Variations in TSM Concentration in the Hongze Lake

The Hongze Lake is an overwater lake with a 35-day water change cycle. The water quality concentration varies greatly throughout the year. Figure 8 shows the seasonal variations in the TSM in the Hongze Lake. The average result for the season was obtained by averaging the corresponding seasonal image data for all years. The concentration of TSM was highest in winter and lowest in autumn. Among them, there was little difference in the concentration of TSM in the entire lake in spring, and the concentration was lower in the west of the Lihe Bay. In summer, the concentration in the central area of the Huaihe Bay and the estuary of the Huai River was higher, and the concentration in the western part of the Lihe Bay was lower. In autumn, the areas with low concentrations of TSM were mainly Chengzi Bay and the western and northern areas of the Lihe Bay, where the concentration of the Huai Lake was more evenly distributed. In winter, the TSM concentration was higher in most areas of the Huaihe Bay and in the southern part of the Lihe Lake Bay.
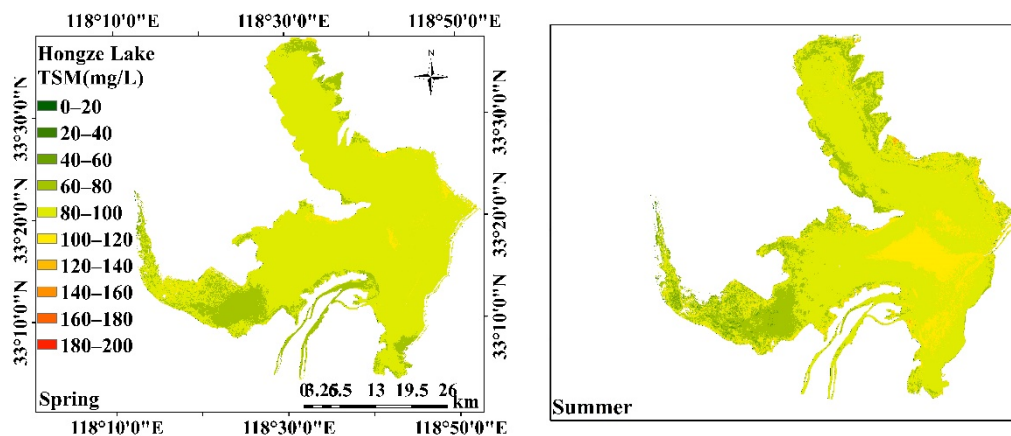
Figure 8. *Cont.*
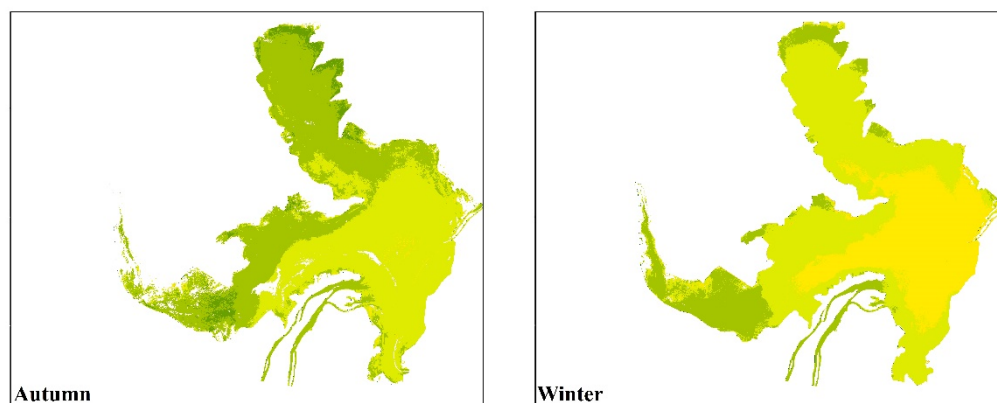
Figure 8. Seasonal changes in the TSM concentration in the Hongze Lake.

4. Discussion

4.1. Suitability and Uncertainty of TSM Estimation Results

Long-term changes to the TSM pattern were clearly identified and quantified using Landsat images, leading to several findings in the Hongze Lake. However, the question remains as to whether the Landsat satellites are suitable for modeling-derived TSM, and the uncertainty of the TSM-derived model is not yet known.

Landsat satellite is a remote sensing satellite with the longest time span of existing satellites in the world. It can monitor the water quality of lakes for up to 40 years, and has incomparable advantages over other satellites. Because its time resolution is not as high as that of MODIS satellites, it cannot quickly reflect the changes in lake water quality over a short time, but it can meet the needs of inter-annual change analysis. The water quality of the Hongze Lake has been affected by social and economic development and human activities in recent decades. Therefore, Landsat data is the best choice for long-term water quality analysis. The water quality of the different areas of the Hongze Lake was quite different. The 30 m spatial resolution of the Landsat satellite could provide detailed information on changes in TSM concentration. A number of recent studies have shown that Landsat archives can be used to monitor water parameters over multiple decades [46,47]. In this study, TM and OLI data were simulated using the measured data according to the spectral response function, and the remote sensing estimation model of TSM concentration in the Hongze Lake was constructed. Based on the above analysis, the two models had a high accuracy and could meet the lake water quality monitoring requirements. Further, the consistency analysis of the two datasets further proved that the Landsat series data are suitable for the long-term serial analysis of TSM concentrations in the Hongze Lake.

The concentration range of TSM at the sampling points in this study was from 11.53 mg/L to 86.80 mg/L. Although the TSM estimations from images in the Hongze Lake exceeded the maximum in some areas, most estimations were less than 86.80 mg/L. Even if some high-concentration in situ data were added to further calibrate the model, the overall concentration would change, but the spatial-temporal patterns and dynamics trends would stay the same. This is especially true when considering similar sediment properties over different years in a relatively small region. Therefore, we were able to use the TSM-derived model to map and analyze long-term TSM distribution patterns in the Hongze Lake using Landsat images. Notably, this study used the measured data from the Hongze Lake to construct an empirical model for the remote sensing estimation of TSM concentrations in the Hongze Lake. Although the near-infrared band were used to estimate TSM concentration in inland lakes, the model parameters had to be recalibrated. Therefore, the model constructed in this study was suitable for the evaluation of TSM concentrations in the Hongze Lake.

4.2. Analysis of Influencing Factors on Inter-annual Variations in TSM Concentration in the Hongze Lake

The factors influencing the Hongze Lake water quality were complex. Because of the fast water exchange rate, the Hongze Lake is strongly affected by the input from upstream Huai River, as well as by human influence. As shown in Figure 9, the wind speed in the Hongze Lake area showed a downward trend from 1984 to 2019. According to the results of previous studies, wind speed can affect the TSM concentration in water bodies. As wind speeds rise, the resuspension of sediments in shallow lakes eventually leads to higher concentrations of TSM. There was a small correlation in the fitting relationship between wind speed and the concentration of TSM in this study, indicating that the concentration of TSM in the Hongze Lake was less affected by wind speed during long-term inter-annual changes. The reduction in wind speed did not lead to a reduction in TSM concentration. Increased in precipitation dilutes the lake TSM concentration, causing the concentration to decrease. There was no obvious increase or decrease in precipitation in the Hongze Lake. Additionally, there was no significant correlation between rainfall and the changes in TSM concentration. This showed that the TSM concentration in the Hongze Lake was less affected by rainfall. In summary, it is clear that the inter-annual variation of TSM in the Hongze Lake was weakly affected by meteorological factors.
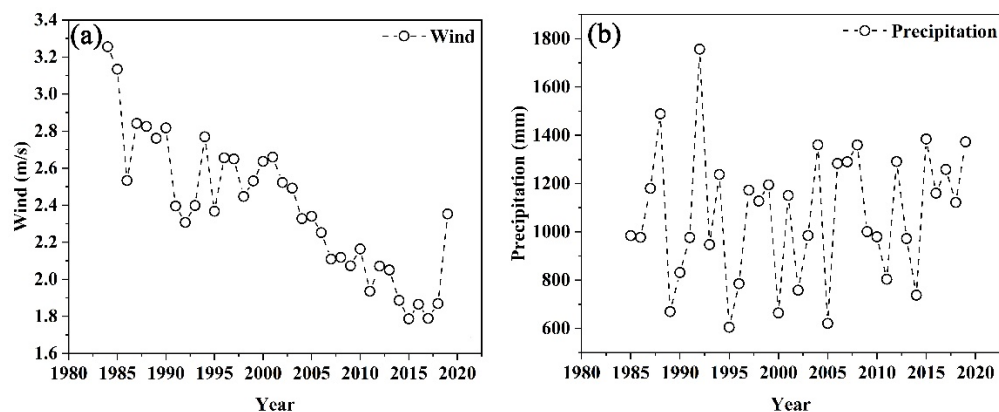
Figure 9. (**a**) Wind speed changes from 1984 to 2019; (**b**) precipitation changes from 1984 to 2019.

According to reports, the 2007 discovery of sand-bearing layers in the main stream of the Huai River and Hongze Lake in Huai'an attracted many profit-driven illegal sand mining boats to the lake area. The number and scale of the boats engaged in illegal sand mining activities increased yearly thereafter. In 2014, relevant state departments issued a notice prohibiting sand mining in the waters of the Hongze Lake. The TSM concentration in the Hongze Lake increased sharply in 2007, mainly as a result of the large sand mining vessels collecting sand layers with diameters of approximately 100 m, which caused turbidity in the surrounding water. When sand mining started to decline in 2014, the concentration dropped significantly. This shows that sand mining was the main reason for the continuous increase in the concentration of TSM in the Hongze Lake after 2007.

Social and economic development and human activities affect the water quality of lakes. Wastewater from industrial development, sewage from farmland irrigation, and domestic sewage are important causes of lake pollution. Since data such as sewage discharge are not easy to obtain, population and GDP are often used as important indicators to measure social development, and are often used to analyze the impacts of human activities on lake pollution [5]. The Hongze Lake is located in Jiangsu, the western wetland area is located in Suqian City, and the rest of the area is mainly located in Huai'an. Therefore, the population and GDP data of Huai'an City over the years were selected to analyze the impact on the TSM concentration in the Hongze Lake. As shown in Figure 10c,d, there is no correlation between the two and the concentration of TSM, indicating that the development

of society and economy has little effect on the inter-annual variation in the concentration of TSM in the Hongze Lake.
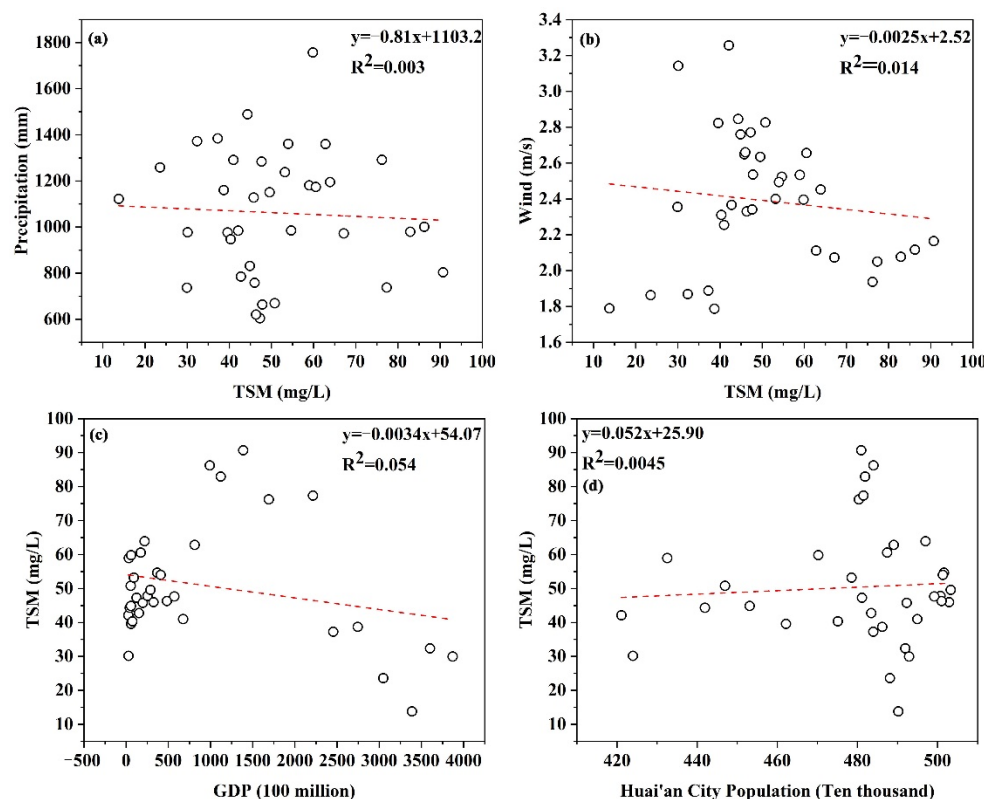
Figure 10. (**a**) Linear relationship between TSM and precipitation; (**b**) linear relationship between TSM and wind speed; (**c**) linear relationship between TSM and GDP; (**d**) linear relationship between TSM and population.

4.3. Potential Factors for Seasonal Changes in TSM

Daily meteorological data from 1984 to 2019 were averaged on a monthly basis to analyze whether seasonal changes in the TSM concentration in the Hongze Lake were affected by climatic factors. As can be seen from Figure 11, the wind speed was relatively high from February to May and reached its maximum in March. From September to December, the wind speed was low, being mainly high in spring and low in summer and autumn. Fitting the average TSM concentration of the Hongze Lake with the wind speed over the 12 months shows that there is no significant correlation trend. The maximum rainfall occurs in July, and the lowest rainfall occurs in December, with high rainfall in spring and summer and low rainfall in autumn and winter. We then calculated the average value of rainfall by month and performed a fitting analysis of the results and TSM. Notably, the summer rainfall (June, July, and August) is marked in red in Figure 12 and does not participate in the fitting. At this time, the fitting accuracy R^2 reached 0.50. The results showed that, except for summer, the TSM concentration and precipitation in the Hongze Lake showed an obvious negative correlation. The higher the precipitation, the lower the TSM concentration. The reason summer was excluded from analysis was mainly because the Hongze Lake water change cycle is very short. In summer, the upper reaches of the Huai River have much precipitation and occasional flooding, which introduces many pollutants into the Hongze Lake. Therefore, the influence of summer rainfall was analyzed separately to reduce the impact of upstream water. According to existing statistical data and research, the Huaihe River flooded approximately 16 times during the summer between 1984 and 2019. The specific dates are shown in Table 1.
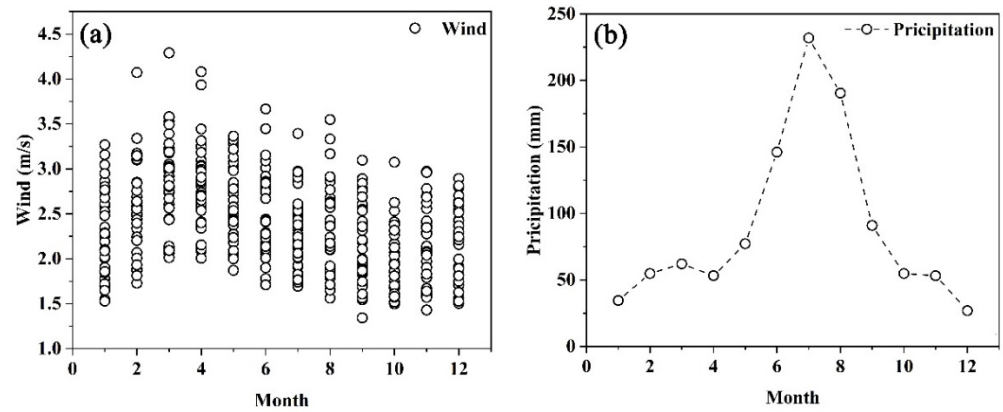
Figure 11. (**a**,**b**) Monthly changes in wind speed and precipitation.
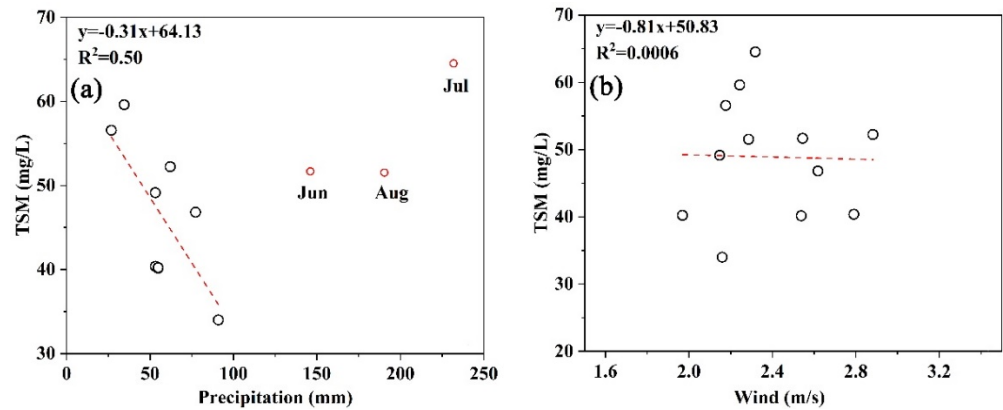
Figure 12. (**a**) Linear relationship between TSM and precipitation; (**b**) linear relationship between TSM and wind speed.

Table 1. Flood times of the Huai River.

Year	Month	Year	Month
1984	6, 7, 8, 9, 10	2000	7
1985	5, 10	2001	7
1986	7, 9	2003	6, 7
1987	El Nino	2005	7
1991	5, 6, 7, 8	2007	6, 7
1996	8, 10	2009	El Nino
1997	7, 8	2011	8
1998	8	2019	8

Flooding dates are mainly concentrated in June, July, and August. Flooding from the Huai River into the Hongze Lake resulted in a large amount of TSM from the erosion of water and soil, and which subsequently increased the TSM concentration of the Hongze Lake. Therefore, despite the high precipitation in the Hongze Lake in summer, the concentration of TSM would still be relatively high. Based on this, the image of the Hongze Lake on a sunny day after heavy rainfall in the upper reaches of the Huai River was selected to analyze the impact of the Huai River's input on the Hongze Lake. The selected image date was 21 July 2017. According to meteorological data (http://data.cma.cn/, accessed on 9 October 2021), heavy precipitation occurred in the upper reaches of the Huai River from 19 July to 20 July. As can be seen from Figure 13, there were obvious plumes in the estuary of the Huai River, and the TSM concentration was higher than that of other areas, which was the main reason for the high TSM concentration in the Hongze Lake in summer.
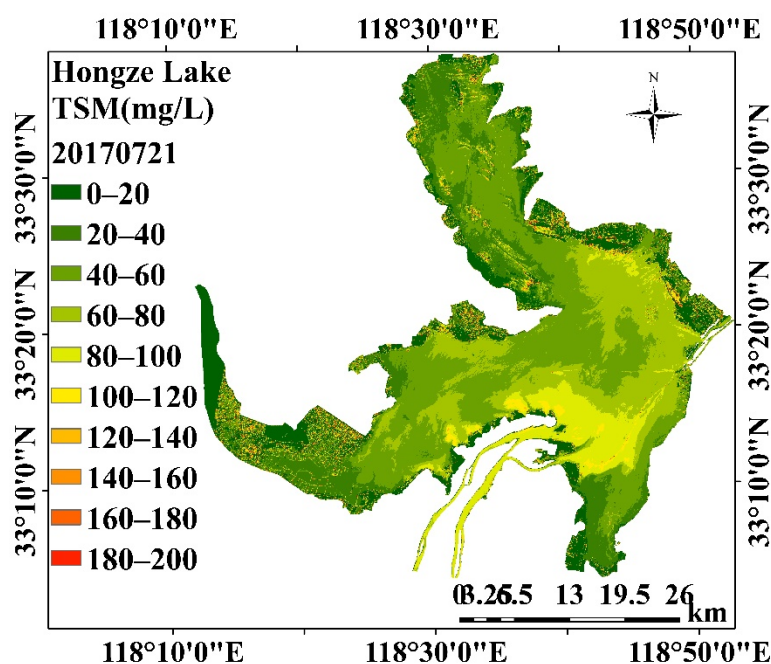
Figure 13. TSM distribution in the Hongze Lake on 21 July 2017.

4.4. Implications for the Hongze Lake Water Quality Monitoring and Ecosystem Restoration

Although the Landsat series satellites are land satellites with no specific characteristic bands with traditional water color sensors, this study showed that it is feasible to use Landsat series data to estimate TSM concentrations in the Hongze Lake in the past 35 years. The estimation results of different sensors had a high consistency, which was suitable for long-term water quality change research. However, the time resolution of the Landsat satellite is low, and the transit period is 16 days, which is not sufficient for the study of short-term lake water quality changes, especially for the plume monitoring of the river into the lake after heavy rains. However, data such as MODIS and GOCI have high temporal resolutions, but low spatial resolutions. A small plume cannot reflect obvious details. Therefore, Landsat data can be fused with data such as MODIS to simultaneously achieve high temporal and spatial resolutions.

Based on the inter-annual variation trend of TSM concentration in the Hongze Lake, the climate had a small impact on the TSM concentration, while human activities, such as sand mining, had a greater impact. Sand mining activities threatened to significantly increase TSM concentrations and severely damage the ecological environment of the Hongze Lake. Therefore, it is necessary to maintain a strict management system for sand mining in the Hongze Lake to avoid the deterioration of the water quality.

The TSM concentration varied seasonally; it was high in summer and winter and low in spring and autumn. The concentration of TSM in the Hongze Lake remained high in summer, even with increased precipitation. The input from the Huai River was the main reason for the TSM increase. In summer, the concentration of TSM in the Huai River's estuary was significantly higher than in other areas of the lake because the Hongze Lake is an important flood discharge lake. In summer, the upstream discharge from the Huai River added a large amount of sediment into the Hongze Lake, resulting in a significantly higher TSM concentration in the Huai River estuary and the Huaihe Bay than in surrounding areas. Whether the brought-in sediment may be exported from the lake via rivers or it may settle into the Hongze Lake, further affecting the water quality. Therefore, more in-depth research is required. A short-term excessive increase in the concentration of TSM can greatly harm aquatic organisms. River discharge needs to be monitored by the government and other regulatory departments to reduce the risk of water pollution. Therefore, specific measures to prevent the concentration of TSM in the Hongze Lake from increasing in summer are

needed to control upstream emissions; these may include reducing soil erosion, controlling pollutant discharge, and multiple small discharges.

5. Conclusions

In this study, we established a satellite TSM model suitable for the Hongze Lake based on Landsat TM and OLI, with high model accuracy. The analysis of the consistency of the OLI and TM monitoring results showed that the multiple sensors of Landsat could be used to monitor the lake water quality over a long time.

From 1984 to 2006, the TSM concentration in the Hongze Lake increased slowly. In 2007, the TSM concentration increased sharply and lasted until 2013, with the highest value being 100.18 mg/L in 2010. The concentration dropped sharply in 2014 and was relatively low until 2019. The concentration of TSM in the Huaihe Bay was the highest, while the TSM concentration in the Chengzi Bay was the lowest. According to the analysis of meteorological and human factors, the abnormal increase in the concentration of TSM from 2007 to 2013 was mainly caused by large-scale sand mining activities. The TSM concentration was the highest in winter, followed by summer, and the lowest in autumn. In summer, the high concentration was mainly due to the discharge from the Huai River, which led to high concentrations, while in the other seasons, the precipitation had a greater effect.

This article analyzed the inter-annual variation of TSM concentrations in the Hongze Lake and the influencing factors, which would help to provide a reference for local authorities to protect the water ecological environment of the Hongze Lake. The improved availability of coupled field and satellite observations bearing information on water optics and compositions is required to provide more details about TSM regulation in this region in the context of environmental changes.

Author Contributions: C.D. and K.S. conceived and designed the method and the experiments. C.D., N.L., C.Y. and J.P. conducted the field experiments and investigations. C.D., Y.G. and Y.L. (Yunmei Li) performed data processing and analysis. C.D. wrote the original manuscript. K.S., Y.L. (Yuan Li) and H.L. revised the manuscript. C.D. conducted the project administration and funding acquisition. All authors have read and agreed to the published version of the manuscript.

Conflicts of Interest: The authors declare no conflict of interest.

Appendix A

Table A1. Valid Landsat images in the period of 1984–2019.

Year	January	February	March	April	May	June	July	August	Sepetember	October	November	December
1984					1					1		
1985				1							2	1
1986		1									1	2
1987		1							1		2	1
1988	1				1	1	1		1	2	2	1
1989			2	2		1		1	1	2	1	1
1990					1	1		1		2		
1991		2				1		1				

Table A1. *Cont.*

Year	January	February	March	April	May	June	July	August	Sepetember	October	November	December
1992		1		1	1					1	1	1
1993		1		1						1	1	1
1994				1	1		2		1			
1995	2		1	1	1							1
1996		1			1							2
1997				1		1				1		
1998				1					1	2	3	2
1999				1					1			2
2000		1		1	2					1		
2001			1	1	1						2	
2002			1				2		1	1		
2003		1	1				1			1		1
2004		1		1						1	2	2
2005		1				1				2	1	
2006			1	1	2					1		
2007	1		1				1					
2008							1					1
2009			2	2				1		1		
2010							1					1
2011	2	1							1			
2013				1				2			1	1
2014	2			1	1	1				1	1	1
2015				1						1	1	1
2016				1			1			1		
2017					1		1					1
2018				1						2	1	1
2019			1				1					

References

1. Cai, Y.; Ke, C.-Q.; Shen, X. Variations in water level, area and volume of Hongze Lake, China from 2003 to 2018. *J. Great Lakes Res.* **2020**, *46*, 1511–1520. [CrossRef]
2. Wu, Y.; Dai, R.; Xu, Y.; Han, J.; Li, P. Statistical assessment of water quality issues in Hongze Lake, China, related to the operation of a water diversion project. *Sustainability* **2018**, *10*, 1885. [CrossRef]
3. Zhang, M.; Tang, J.; Dong, Q.; Song, Q.; Ding, J. Retrieval of total suspended matter concentration in the Yellow and East China Seas from MODIS imagery. *Remote Sens Environ.* **2010**, *114*, 392–403. [CrossRef]
4. Miller, R.L.; McKee, B.A. Using MODIS Terra 250 m imagery to map concentrations of total suspended matter in coastal waters. *Remote Sens Environ.* **2004**, *93*, 259–266. [CrossRef]
5. Du, C.; Li, Y.; Wang, Q.; Liu, G.; Zheng, Z.; Mu, M.; Li, Y. Tempo-spatial dynamics of water quality and its response to river flow in estuary of Taihu Lake based on GOCI imagery. *Environ. Sci. Pollut. Res.* **2017**, *24*, 28079–28101. [CrossRef] [PubMed]
6. Qin, B.; Yang, L.; Chen, F.; Zhu, G.; Zhang, L.; Chen, Y. Mechanism and control of lake eutrophication. *Chin. Sci. Bull.* **2006**, *51*, 2401–2412. [CrossRef]
7. Qin, B.; Zhu, G. The nutrient forms, cycling and exchange flux in the sediment and overlying water system in lakes from the middle and lower reaches of Yangtze River. *Sci. China Ser. D* **2006**, *49*, 1. [CrossRef]
8. Liu, H.; Li, Q.; Shi, T.; Hu, S.; Wu, G.; Zhou, Q. Application of sentinel 2 MSI images to retrieve suspended particulate matter concentrations in Poyang Lake. *Remote Sens.* **2017**, *9*, 761. [CrossRef]
9. Ciancia, E.; Campanelli, A.; Lacava, T.; Palombo, A.; Pascucci, S.; Pergola, N.; Pignatti, S.; Satriano, V.; Tramutoli, V. Modeling and multi-temporal characterization of total suspended matter by the combined use of Sentinel 2-MSI and Landsat 8-OLI data: The Pertusillo Lake case study (Italy). *Remote Sens.* **2020**, *12*, 2147. [CrossRef]
10. Cao, Z.; Duan, H.; Feng, L.; Ma, R.; Xue, K. Climate- and human-induced changes in suspended particulate matter over Lake Hongze on short and long timescales. *Remote Sens. Environ.* **2017**, *192*, 98–113. [CrossRef]
11. Usali, N.; Ismail, M.H. Use of remote sensing and GIS in monitoring water quality. *J. Sustain. Dev.* **2010**, *3*, 228. [CrossRef]
12. Topp, S.N.; Pavelsky, T.M.; Jensen, D.; Simard, M.; Ross, M.R. Research trends in the use of remote sensing for inland water quality science: Moving towards multidisciplinary applications. *Water* **2020**, *12*, 169. [CrossRef]
13. Flores-Anderson, A.I.; Griffin, R.; Dix, M.; Romero-Oliva, C.S.; Ochaeta, G.; Skinner-Alvarado, J.; Ramirez Moran, M.V.; Hernandez, B.; Cherrington, E.; Page, B.; et al. Hyperspectral satellite remote sensing of water quality in Lake Atitlán, Guatemala. *Front. Environ. Sci.* **2020**, *8*, 7. [CrossRef]
14. Chawla, I.; Karthikeyan, L.; Mishra, A.K. A review of remote sensing applications for water security: Quantity, quality, and extremes. *J. Hydrol.* **2020**, *585*, 124826. [CrossRef]
15. Shi, K.; Zhang, Y.; Song, K.; Liu, M.; Zhou, Y.; Zhang, Y.; Li, Y.; Zhu, G.; Qin, B. A semi-analytical approach for remote sensing of trophic state in inland waters: Bio-optical mechanism and application. *Remote Sens. Environ.* **2019**, *232*, 111349. [CrossRef]
16. Eraso, R.; de Lourdes Galo, M.; Alcântara, E.; Shimabukuro, M.; Carmo, A. Locally tuned model to map the chlorophyll-a and the trophic state in Porto Primavera reservoir using MODIS/Terra images. *Modeling Earth Syst. Environ.* **2018**, *4*, 39–47. [CrossRef]
17. Yu, X.; Lee, Z.; Shen, F.; Wang, M.; Wei, J.; Jiang, L.; Shang, Z. An empirical algorithm to seamlessly retrieve the concentration of suspended particulate matter from water color across ocean to turbid river mouths. *Remote Sens. Environ.* **2019**, *235*, 111491. [CrossRef]

18. Pan, Y.; Shen, F.; Wei, X. Fusion of Landsat-8/OLI and GOCI Data for Hourly Mapping of Suspended Particulate Matter at High Spatial Resolution: A Case Study in the Yangtze (Changjiang) Estuary. *Remote Sens.* **2018**, *10*, 158. [CrossRef]

19. Du, C.; Wang, Q.; Li, Y.; Lyu, H.; Zhu, L.; Zheng, Z.; Wen, S.; Liu, G.; Guo, Y. Estimation of total phosphorus concentration using a water classification method in inland water. *Int. J. Appl. Earth Obs.* **2018**, *71*, 29–42. [CrossRef]

20. Shi, K.; Zhang, Y.; Zhu, G.; Qin, B.; Pan, D. Deteriorating water clarity in shallow waters: Evidence from long term MODIS and in-situ observations. *Int. J. Appl. Earth Obs.* **2018**, *68*, 287–297. [CrossRef]

21. Buznikov, A.A.; Lakhtanov, G.A.; Laine, P.; Minkkinen, P.; Rakushin, P.B. Development of water quality models for remote sensing of the Saimaa lake system. *Earth Obs. Remote Sens.* **2001**, *16*, 997–1006.

22. Zhang, Y.; Huang, Z.; Fu, D.; Tsou, J.Y.; Jiang, T.; Liang, X.S.; Lu, X. Monitoring of chlorophyll-a and sea surface silicate concentrations in the south part of Cheju island in the East China sea using MODIS data. *Int. J. Appl. Earth Obs.* **2018**, *67*, 173–178. [CrossRef]

23. Chen, J.; Zhu, W.-N.; Tian, Y.Q.; Yu, Q. Estimation of Colored Dissolved Organic Matter From Landsat-8 Imagery for Complex Inland Water: Case Study of Lake Huron. *IEEE Trans. Geosci. Remote Sens.* **2017**, *55*, 2201–2212. [CrossRef]

24. Engel, A.; Bracher, A.; Dinter, T.; Endres, S.; Grosse, J.; Metfies, K.; Peeken, I.; Piontek, J.; Salter, I.; Nöthig, E.-M. Inter-Annual Variability of Organic Carbon Concentration in the Eastern Fram Strait During Summer (2009–2017). *Front. Mar. Sci.* **2019**, *6*, 187. [CrossRef]

25. Zheng, Z.; Ren, J.; Li, Y.; Huang, C.; Liu, G.; Du, C.; Lyu, H. Remote sensing of diffuse attenuation coefficient patterns from Landsat 8 OLI imagery of turbid inland waters: A case study of Dongting Lake. *Sci. Total Environ.* **2016**, *573*, 39–54. [CrossRef] [PubMed]

26. Ogashawara, I. Advances and limitations of using satellites to monitor cyanobacterial harmful algal blooms. *Acta Limnol. Bras.* **2019**, *31*. [CrossRef]

27. Zhou, B.; Shang, M.; Feng, L.; Shan, K.; Feng, L.; Ma, J.; Liu, X.; Wu, L. Long-term remote tracking the dynamics of surface water turbidity using a density peaks-based classification: A case study in the Three Gorges Reservoir, China. *J. Ecol. Indic.* **2020**, *116*, 106539. [CrossRef]

28. Pham, Q.; Ha, N.; Pahlevan, N.; Oanh, L.; Nguyen, T.; Nguyen, N.J.R.S. Using Landsat-8 Images for Quantifying Suspended Sediment Concentration in Red River (Northern Vietnam). *Remote Sens.* **2018**, *10*, 1841. [CrossRef]

29. Tian, L.; Wai, O.W.H.; Chen, X.; Li, W.; Li, J.; Li, W.; Zhang, H. Retrieval of total suspended matter concentration from Gaofen-1 Wide Field Imager (WFI) multispectral imagery with the assistance of Terra MODIS in turbid water—Case in Deep Bay. *Int. J. Remote Sens.* **2016**, *37*, 3400–3413. [CrossRef]

30. Zhan, W.; Wu, J.; Wei, X.; Tang, S.; Zhan, H.J.C.S.R. Spatio-temporal variation of the suspended sediment concentration in the Pearl River Estuary observed by MODIS during 2003–2015. *Cont. Shelf Res.* **2018**, *172*, 22–32. [CrossRef]

31. Dekker, A.G.; Vos, R.; Peters, S. Analytical algorithms for lake water TSM estimation for retrospective analyses of TM and SPOT sensor data. *Int. J. Remote Sens.* **2002**, *23*, 15–35. [CrossRef]

32. Zheng, Z.; Li, Y.; Guo, Y.; Xu, Y.; Liu, G.; Du, C. Landsat-Based Long-Term Monitoring of Total Suspended Matter Concentration Pattern Change in the Wet Season for Dongting Lake, China. *Remote Sens.* **2015**, *7*, 13975–13999. [CrossRef]

33. Zhang, Y.; Shi, K.; Zhang, Y.; Moreno-Madriñán, M.J.; Zhu, G.; Zhou, Y.; Yao, X. Long-term change of total suspended matter in a deep-valley reservoir with HJ-1A/B: Implications for reservoir management. *Environ. Sci. Pollut. Res.* **2019**, *26*, 3041–3054. [CrossRef]

34. Mao, Z.; Chen, J.; Pan, D.; Tao, B.; Zhu, Q. A regional remote sensing algorithm for total suspended matter in the East China Sea. *Remote Sens. Environ.* **2012**, *124*, 819–831. [CrossRef]

35. Shi, K.; Zhang, Y.; Zhu, G.; Liu, X.; Zhou, Y.; Xu, H.; Qin, B.; Liu, G.; Li, Y. Long-term remote monitoring of total suspended matter concentration in Lake Taihu using 250 m MODIS-Aqua data. *Remote Sens. Environ.* **2015**, *164*, 43–56. [CrossRef]

36. Lymburner, L.; Botha, E.; Hestir, E.; Anstee, J.; Sagar, S.; Dekker, A.; Malthus, T. Landsat 8: Providing continuity and increased precision for measuring multi-decadal time series of total suspended matter. *Remote Sens. Environ.* **2016**, *185*, 108–118. [CrossRef]

37. Yang, H.; Kong, J.; Hu, H.; Du, Y.; Gao, M.; Chen, F. A Review of Remote Sensing for Water Quality Retrieval: Progress and Challenges. *Remote Sens.* **2022**, *14*, 1770. [CrossRef]

38. Lei, S.; Wu, D.; Li, Y.; Wang, Q.; Huang, C.; Liu, G.; Zheng, Z.; Du, C.; Mu, M.; Xu, J.; et al. Remote sensing monitoring of the suspended particle size in Hongze Lake based on GF-1 data. *J. Int. J. Remote Sens.* **2019**, *40*, 3179–3203. [CrossRef]

39. Tang, J.-W.; Tian, G.-L.; Wang, X.-Y.; Wang, X.-M.; Song, Q.-J. The methods of water spectra measurement and analysis I: Above-water method. *Int. J. Remote Sens.* **2004**, *8*, 37–44.

40. Dekker, A.; Vos, R.; Peters, S. Comparison of remote sensing data, model results and in situ data for total suspended matter (TSM) in the southern Frisian lakes. *Sci. Total Environ.* **2001**, *268*, 197–214. [CrossRef]

41. Racetin, I.; Krtalic, A.; Srzic, V.; Zovko, M. Characterization of short-term salinity fluctuations in the Neretva River Delta situated in the southern Adriatic Croatia using Landsat-5 TM. *Ecol. Indic.* **2020**, *110*, 105924. [CrossRef]

42. Wu, C.F.; Wu, J.P.; Qi, J.G.; Zhang, L.; Huang, H.Q.; Lou, L.P.; Chen, Y.X. Empirical estimation of total phosphorus concentration in the mainstream of the Qiantang River in China using Landsat TM data. *Int. J. Remote Sens.* **2010**, *31*, 2309–2324. [CrossRef]

43. Moses, W.J.; Gitelson, A.A.; Perk, R.L.; Gurlin, D.; Rundquist, D.C.; Leavitt, B.C.; Barrow, T.M.; Brakhage, P. Estimation of chlorophyll-a concentration in turbid productive waters using airborne hyperspectral data. *J. Water Res.* **2012**, *46*, 993–1004. [CrossRef]

44. Baban, S.M. Detecting water quality parameters in the Norfolk Broads, UK, using Landsat imagery. *Int. J. Remote Sens.* **1993**, *14*, 1247–1267. [CrossRef]

45. Alcântara, E.; Curtarelli, M.; Kampel, M.; Stech, J. Spatiotemporal total suspended matter estimation in Itumbiara reservoir with Landsat-8/OLI images. *Int. J. Cartogr.* **2016**, *2*, 148–165. [CrossRef]

46. Zhu, Z. Change detection using landsat time series: A review of frequencies, preprocessing, algorithms, and applications. *ISPRS J. Photogramm. Remote Sens.* **2017**, *130*, 370–384. [CrossRef]

47. Cao, Z.; Ma, R.; Duan, H.; Pahlevan, N.; Melack, J.; Shen, M.; Xue, K. A machine learning approach to estimate chlorophyll-a from Landsat-8 measurements in inland lakes. *Remote Sens. Environ.* **2020**, *248*, 111974. [CrossRef]